

Can statistical methods optimize complex multicomponent mixtures for sintering ceramic granular materials? A case of success with synthetic aggregates

José Manuel Moreno-Maroto^{a,d,*}, Carlos Javier Cobo-Ceacero^a, Antonio Conde-Sánchez^b, Ana M. Martínez-Rodríguez^b, Beatriz González-Corrochano^a, Jacinto Alonso-Azcárate^c, Manuel Uceda-Rodríguez^a, Ana B. López^a, Carmen Martínez-García^a, Teresa Cotes-Palomino^a

^a University of Jaén. Department of Chemical, Environmental and Materials Engineering, Higher Polytechnic School of Linares, Scientific and Technological Campus of Linares, 23700, Linares (Jaén), Spain

^b University of Jaén. Department of Statistics and Operations Research. Campus of Las Lagunillas, 23071, Jaén, Spain

^c University of Castilla-La Mancha. Department of Physical Chemistry, Faculty of Environmental Sciences and Biochemistry, Avenida Carlos III, s/n, 45071, Toledo, Spain

^d Department of Geology and Geochemistry, Faculty of Sciences, Autonomous University of Madrid, Cantoblanco, 28049, Madrid, Spain

ARTICLE INFO

Keywords:

Aggregate
Kaolin
Pyrite
Na₂CO₃
Organic carbon
Design of experiments

ABSTRACT

The relationship between the proportions of multicomponent mixtures with the technological properties of ceramic granular materials (synthetic aggregates) has been studied using statistical methods. The four phases involved in the formulations have been: kaolin (K) as aluminosilicate source; cork powder (C) as organic carbon source; sodium carbonate (N) as flux and pyrite (P) as source of iron and sulfur. The Mixture Experiments - Design of Experiments (ME-DOE) has been the statistical methodology applied from the initial configuration of the 36 starting formulations to the final validation of the models and optimums. After granulation, artificial aggregates have been obtained by sintering in a rotary kiln, and their main technological properties have been determined. Bloating index (BI), particle density (ρ_{td}), water absorption (WA₂₄) and crushing strength (S) were selected as the four key characteristics to be modeled and optimized, using response surface and effect plots to assess the effect of K, C, N and P on such properties. 32 out of 36 starting varieties met the density criteria for lightweight aggregates. In the optimum formulations obtained, the minimum percentage of K was 83 wt%, so that the variations in the percentages of P, C and N were the critical variables for determining the final properties of the aggregate. The contrast between experimental and estimated data has shown that the models fit adequately, indicating that this type of approach may have enormous potential for future research on artificial aggregates and other ceramic materials.

1. Introduction

The growing human demand for goods makes it increasingly necessary to optimize the resources used in their production. In this way, savings can be made not only economically but also from an environmental perspective, helping to reduce the consumption of natural resources and energy. Such aspects are aligned, for example, with internationally adopted policies on Circular Economy [1,2], the

European Green Deal [3], as well as with several of the Sustainable Development Goals described in the United Nations 2030 Agenda [4].

However, the implementation of new methodologies and raw materials undoubtedly presents the challenge of at least matching the quality and performance of the product obtained with the one it is intended to replace. Thus, the complexity of the processes that occur during manufacturing will increase as the number of variables involved (e.g. number of components) also increases, due to the synergies that

* Corresponding author. University of Jaén. Department of Chemical, Environmental and Materials Engineering, Higher Polytechnic School of Linares, Scientific and Technological Campus of Linares, 23700, Linares (Jaén), Spain.

E-mail addresses: josemanuel.moreno@uam.es (J.M. Moreno-Maroto), cjcobo@ujaen.es (C.J. Cobo-Ceacero), aconde@ujaen.es (A. Conde-Sánchez), ammartin@ujaen.es (A.M. Martínez-Rodríguez), bcorroch@ujaen.es (B. González-Corrochano), jacinto.alonso@uclm.es (J. Alonso-Azcárate), muceda@ujaen.es (M. Uceda-Rodríguez), ablopez@ujaen.es (A.B. López), cmartin@ujaen.es (C. Martínez-García), mtcotes@ujaen.es (T. Cotes-Palomino).

<https://doi.org/10.1016/j.ceramint.2022.09.220>

Received 7 July 2022; Received in revised form 6 September 2022; Accepted 17 September 2022

Available online 22 September 2022

0272-8842/© 2022 The Authors. Published by Elsevier Ltd. This is an open access article under the CC BY-NC-ND license (<http://creativecommons.org/licenses/by-nc-nd/4.0/>).

occur between them. In this sense, the application of statistical methods can be of great help to adjust formulations and manufacturing conditions, and thus optimize the properties of the final product at convenience, without the need to perform an exaggerated number of previous laboratory tests.

The ceramics sector is no stranger to this, and several examples can be found in which statistical approaches have been studied to improve manufacturing processes. Using three raw materials, two natural materials (red clay and kaolin) and a granite sawing waste, Menezes et al. [5] employed the statistical methodology of Mixtures Experiments to maximize the use of such residue in ceramic tile formulations. The regression models obtained were applied to correlate each mixture composition with water absorption, linear firing shrinkage and modulus of rupture. Statistical analysis along with verification tests demonstrated that the models were adequate and useful to optimize the proportion of granite-based waste in the formulations, whose maximum limit was established at 62%.

Arsenović et al. [6,7] investigated the incorporation of various organic and inorganic wastes (sludges, coal dust, fly and landfill ashes, soybean crust, sawdust, sunflower hulls and their ash) in heavy clay to produce ceramic materials, namely tiles, solid bricks and hollow blocks. In the first part of their papers [6], both Response Surface Methodology (RSM) and Second Order Polynomial models (SOP) were applied to assess the impact of the type of residue, its proportion and the sintering temperature on the properties of the final products. The results were satisfactory according to their high predictive capacity and coefficients of determination ($R^2 = 0.896$ – 0.999). The second part of this research [7] focused mainly on certain technological properties, such as shaping moisture, shrinkage, weight loss in Bigot's curve and Pfefferkorn plasticity. Particularly, the type and content of waste and the firing temperature were considered independent variables to analyze their effect on compressive strength, water absorption, firing shrinkage, mass loss and volume mass. First, SOP were used to model, while RSM coupled with Fuzzy Synthetic Evaluation algorithm (FSE) were applied through trapezoidal function to optimize. The optimization results were adequate and met expectations in terms of the application of statistical methods for ceramics.

The examples mentioned above refer to traditional, relatively large ceramic pieces used in construction (bricks, blocks and tiles). However, ceramic granular materials, such as lightweight aggregates (LWAs), are expected to be key players in the construction of the future, not only because of their technological properties that allow better insulation of buildings and lower load bearing capacity [8], but also because they are a potential substitute for natural aggregate, which is the second most consumed raw material by man only behind water [9,10]. The final characteristics that an artificial aggregate produced by sintering (such as LWA) will have, apart from the manufacturing conditions (temperature, firing time, etc.) will depend to a large extent on the composition of the raw materials. Thus, the proportion of aluminosilicates, alkaline and alkaline earth fluxes, iron species and organic carbon are among the variables that can most influence the properties of the final product obtained [11–16]. The complexity in the interaction between them means that, for example, the bloating process of a lightweight aggregate cannot be predicted on the basis of its chemical composition alone [14].

For all these reasons, the application of statistical methods seems to be promising also in the granular ceramics field. However, there is not much previous research on this subject. Hu et al. [17] studied municipal solid waste incineration (MSWI) fly ash, electrolytic manganese residues (EMR) and coal fly ash as raw materials to sinter lightweight aggregates. Based on Uniform Design (UD), a quadratic regression model was deduced to investigate the proportion of each waste in the mixture over the final properties of the LWAs obtained. According to the authors, the data were well fitted by the regressed second-order polynomial models and mixture optimization could be properly conducted. This optimum was set at: EMR = 49.19%, MSWI fly ash = 12.91% and coal fly ash = 37.90%, whose LWA eluates did not involve any risk to the environment

based on its heavy metal concentration after leaching tests.

Wie et al. [18] modeled the manufacturing process (focused on drying, calcination and sintering) of expanded clay LWAs by machine-learning (ML) techniques. First, an $L_{18}(3^6)$ orthogonal array table was designed to obtain 486 data from only 18 laboratory tests. From the data obtained, three ML approaches, specifically linear regression, random forest, and support vector regression (SVR), were applied and their predictive capacity was evaluated by comparing estimated values with those obtained in actual laboratory tests. The results revealed that the best fitting model was the one obtained by SVR and that ML could be applied in LWA investigation.

The present work is intended to deepen in the statistical techniques for the synthesis of ceramic aggregates (lightweight or not). For this purpose, it will be essential to use pure raw materials, whose composition is perfectly defined and which will allow a better understanding of the possible processes occurring during sintering. Mixture Experiments (ME), which is framed within the Design of Experiments (DOE), will be the statistical method used in this research, hereinafter referred to as ME-DOE. These types of methods usually require the application of more complex fits than the linear model, such as quadratic, special cubic or cubic models. Depending on the model considered, a minimum number of samples is required to estimate the model coefficients, something that the ME-DOE itself allows to define. Using those regression models, ME-DOE is expected to determine the effect of the components of the mixtures on the properties of the ceramic materials to be studied, in this case synthetic aggregates.

2. Materials and methods

2.1. Raw materials

This work has investigated the interaction of four components during sintering: pure kaolin (K) as basic aluminosilicate-rich component, cork powder (C) as source of reducing organic carbon, Na_2CO_3 (N) as a flux (PanReac, for analysis, ACS) and FeS_2 (P) as iron donor and source of sulfur gases. Regarding the kaolin (Caobar, S.A., Taracena, Spain), based on laser diffraction tests (Coulter® LSTM 230 equipment), it presented a very fine particle size distribution, with mean size of 8.3 μm and main mode around 4.6 μm (Fig. 1). TOC-analyzer (Shimadzu® TOC-VCSH) tests revealed no carbon content in this clay (Table 1). In terms of chemical composition (Thermo ARL ADVANT'XP Sequential XRF), its two main components are SiO_2 (51%) and Al_2O_3 (35%), with an almost total absence of alkaline and alkaline-earth fluxing elements as well as of iron (only 0.4%). The selection of a clay with these chemical characteristics (composed almost exclusively of Si and Al) was made on purpose in order to control the proportions of iron, sulfur, alkali flux and organic carbon in the mixtures through the incorporation of the additives P, N and C. This would allow the individual effect of these

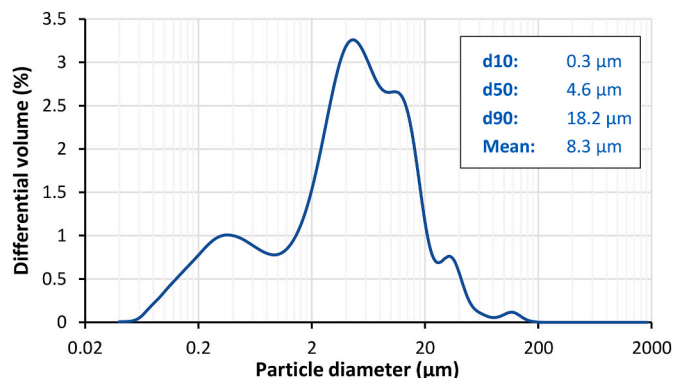


Fig. 1. Particle size distribution of the kaolin used in this research. The x-axis is shown in logarithmic scale.

Table 1

Main characteristics of the kaolin used in this investigation.

Clay name	Carbon content (%)			LOI (%)	Chemical composition, oxides (%)										Mineralogy	
	TC	IC	OC		SiO ₂	Al ₂ O ₃	Fe ₂ O ₃ ^a	Na ₂ O ^a	K ₂ O ^a	MgO ^a	CaO ^a	TiO ₂	SO ₃	P ₂ O ₅	Major	Minor
Kaolin	0.0	0.0	0.0	12.6	50.9	35.0	0.4	0.0	0.4	0.1	0.1	0.1	0.4	0.1	Kaolinite	Quartz, Illite

^a Fluxing oxide.

components during firing, as well as their synergies, to be investigated. The mineralogy studied using a PANalytical® X'Pert Pro MRD diffractometer has shown that the main component in K is kaolinite, with minor proportions of quartz and illite (Table 1).

For its part, P was obtained in the form of pyrite from the Navajún deposit (La Rioja, northern Spain) and subsequently ground below 250 µm with a Restsch® MM 200 ball mill. C is a powdery waste generated in the industrial processing of cork (Eurotapón Núñez, S.L., San Vicente de Alcántara, Spain), which is totally organic, exhibiting a total loss on ignition (LOI = 100%) and a high calorific value ($\sim 3 \times 10^4$ kJ/kg), according to the investigation conducted by Cobo-Ceacero et al. [19] using the same residue.

The thermal behavior of the raw materials was studied in both air and argon atmosphere by simultaneous Differential Thermal Analysis-Thermogravimetric Analysis (DTA-TG). The test conditions were: SETARAM® equipment; max. temperature: 1200 °C; ramp: 10 °C/min; air flow rate: 30 ml/min; Ar flow rate: 40 ml/min. The main results of the DTA-TGA tests will be discussed in connection with those obtained for the sintered materials.

2.2. Preparation of mixtures

The ME-DOE of this research has 4 components (K, C, N and M) and is considered a *Constrained Mixture Experiment* [20]. The starting mixtures (Table 2) were designed using the *mixexp* package of R, specifically through the *Xvert* function [21]. Such formulations were planned in order to estimate a cubic model for each of the fundamental properties of the aggregates, namely their bloating index (*BI*), particle density (ρ_{rd} , also called oven-dry density), water absorption (*WA*₂₄) and crushing strength (*S*).

As shown in Table 2, ME-DOE defined 5 equidistant percentages for the additives C, N and P, whose minimum value was in any case 0 wt%. Their upper limit was set according to operational criteria after preliminary testing. In the case of C, the maximum proportion to be added was 5 wt%, since higher proportions can inhibit volumetric bloating when, for instance, the aim is to obtain expanded lightweight aggregates [15,19]. In the case of sodium carbonate, it has also been set at 5 wt% because it is an additive that tends to favor the melting of the surface of the specimens, making firing difficult, an aspect that agrees with other research [22]. The maximum P amount was set at 15 wt% to minimize the emission of potentially harmful gases, such as SO₂ and SO₃ generated

Table 2Composition and plasticity of the starting mixtures studied. K = kaolin; P = pyrite (FeS₂); C = cork powder (organic matter); N = sodium carbonate (Na₂CO₃).

Components (%)					Plasticity					
Mix.	K	P	C	N	LL	PL	PI	PI/LL	W _{OP} (%)	
P1	100	0	0	0	42.1	22.7	19.5	0.46	33.9	
P2	97.5	0	2.5	0	45.1	24.2	20.9	0.46	36.2	
P3	97.5	0	0	2.5	42.5	22.4	20.1	0.47	33.5	
P4	95	0	5	0	48.1	25.7	22.3	0.46	38.5	
P5	95	0	0	5	42.9	22.1	20.8	0.48	33.1	
P6	95	0	2.5	2.5	45.5	23.9	21.6	0.47	35.8	
P7	95	0	2.5	2.5	45.5	23.9	21.6	0.47	35.8	
P8	92.5	0	5	2.5	48.5	25.5	23.0	0.47	38.0	
P9	92.5	0	2.5	5	45.9	23.6	22.2	0.48	35.3	
P10	90	0	5	5	48.9	25.2	23.7	0.48	37.6	
P11	93.75	3.75	1.25	1.25	42.7	22.7	20.0	0.47	34.0	
P12	91.25	3.75	3.75	1.25	45.8	24.3	21.5	0.47	36.4	
P13	91.25	3.75	1.25	3.75	43.1	22.5	20.7	0.48	33.6	
P14	88.75	3.75	3.75	3.75	46.2	24.0	22.2	0.48	35.9	
P15	92.5	7.5	0	0	39.8	21.5	18.3	0.46	32.1	
P16	90	7.5	0	2.5	40.2	21.2	19.0	0.47	31.7	
P17	90	7.5	2.5	0	43.0	23.2	19.8	0.46	34.6	
P18	87.5	7.5	5	0	46.2	24.8	21.4	0.46	37.1	
P19	87.5	7.5	0	5	40.6	20.9	19.7	0.49	31.3	
P20	85	7.5	5	2.5	46.7	24.5	22.1	0.47	36.7	
P21	85	7.5	2.5	5	43.9	22.6	21.3	0.49	33.7	
P22	82.5	7.5	5	5	47.1	24.2	22.9	0.49	36.2	
P23	86.25	11.25	1.25	1.25	40.5	21.6	18.9	0.47	32.3	
P24	83.75	11.25	3.75	1.25	43.9	23.4	20.5	0.47	34.9	
P25	83.75	11.25	1.25	3.75	41.0	21.3	19.7	0.48	31.9	
P26	81.25	11.25	3.75	3.75	44.3	23.0	21.3	0.48	34.5	
P27	85	15	0	0	37.5	20.3	17.1	0.46	30.4	
P28	82.5	15	2.5	0	41.0	22.1	18.8	0.46	33.1	
P29	82.5	15	0	2.5	37.9	20.0	17.9	0.47	29.9	
P30	80	15	5	0	44.4	24.0	20.5	0.46	35.8	
P31	80	15	2.5	2.5	41.4	21.8	19.6	0.47	32.6	
P32	80	15	2.5	2.5	41.4	21.8	19.6	0.47	32.6	
P33	80	15	0	5	38.4	19.7	18.7	0.49	29.5	
P34	77.5	15	2.5	5	41.9	21.5	20.4	0.49	32.1	
P35	77.5	15	5	2.5	44.9	23.6	21.3	0.47	35.3	
P36	75	15	5	5	45.4	23.3	22.1	0.49	34.8	

in the thermal oxidation of pyrite [23]. Consequently, the amount of kaolin added was set according to those of the other components, ranging from a maximum of 100 wt% (P1 in Table 2) to a minimum of 75 wt% (P36 in Table 2).

2.3. Synthesis of the ceramic aggregates

The optimum water content (W_{OP}) for extrusion and pelletizing was added to each of the mixtures in Table 2. Previously, the Atterberg liquid limit (LL; [24]) and the plastic limit (PL; [25]) were determined, as well as the difference between them (plasticity index, PI), so W_{OP} was calculated as follows: $W_{OP} = 1.495 \times PL$ [25]. To ensure that the water distribution in mixture was homogeneous, it was kept for 24 h under sealed conditions. Then, it was mechanically extruded (Nannetti® pneumatic extruder) and round pellets of approximately $\varnothing = 9.3$ mm were manually shaped. The granules were dried for 48 h, first at room temperature and the last 24 h in an oven at 105 °C.

The final ceramic aggregates were obtained in the laboratory by sintering, emulating the equipment (firing in Nannetti® TOR-R 120–14 tubular rotary kiln) and firing conditions (2 min preheating + 10 min at maximum temperature) normally used on an industrial scale. The temperature was set for each mixture, following the criterion of the maximum operationally feasible, so above the specimens could stick to each other or to the kiln tube.

2.4. Aggregate characterization

A batch consisting of 25 specimens was selected to determine the total LOI during firing (LOI_{firing}) and during preheating ($LOI_{preheating}$), as well as the percentage of bloating index (BI) based on the measurement of the granule diameter before and after firing [26].

Water absorption for 24 h of soaking (WA_{24} ; [27]), apparent density (ρ_a ; [27]), particle density (ρ_{rd} ; oven-dry density in [27]) and loose bulk density (ρ_b ; [28]), were also determined. Solid phase density (ρ_{solid}), required to estimate porosity, was calculated based on Eq. (1):

$$\rho_{solid} = 2.6 \times [K/(K + P)] + 5 \times [P/(K + P)] \quad (1)$$

where:

K is the % of kaolin; P is the % of pyrite; 2.6 (g/cm³) is the common ρ_{solid} of a sintered aggregate [29,30]; 5 (g/cm³) is the approximate ρ_{solid} of pyrite and Fe₂O₃ (the latter is a result of pyrite oxidation). C and N has not been considered because they cannot significantly affect ρ_{solid} (their proportion in mixtures is low and they tend to decompose thermally).

Based on ρ_a , ρ_{rd} and ρ_{solid} , porosity (total (P_T), open (P_O) and closed (P_C)) was calculated [31,32]. Individual aggregate crushing strength (S) was determined with a Nannetti®FM 96 press as the average value resulting from testing 25 specimens according to Yashima et al. [33] and Li et al. [34].

2.5. Statistical analysis, optimization and validation

As indicated in section 2.2, the ME-DOE applied in this research focused on the study of the relationship of compositional variables (K, P, C and N) with the technological properties BI, ρ_{rd} , WA_{24} and S, using the software R for this purpose. Cubic, special cubic, quadratic and linear regression models have been computed, so that after comparing them, the most appropriate one has been selected on the basis of statistical criteria, such as ANOVA.

The definitive models were the basis for obtaining effect plots and response surface plots (contour plots). Based on the criteria usually applied for lightweight aggregates, the maximum values of BI, WA_{24} and S have been considered as optimal for optimization, while on the contrary, the minimum ρ_{rd} value has been sought. Once the theoretically optimum mixtures were estimated, they were prepared in the laboratory to manufacture and characterize their corresponding ceramic aggregates

following the same protocols as those indicated in sections 2.3 and 2.4. The validation of the four models obtained (one for each key property) was based on the comparison between the experimental results and those estimated for the optimum formulations.

3. Results and discussion

3.1. Starting characteristics of the aggregates before modeling

3.1.1. General aspects

First, from a rheological point of view, the addition of C, N or P has hardly affected the plasticity of the starting mixtures when compared to the kaolin (P1 in Table 2: LL = 42.1; PI = 19.5; PI/LL = 0.46). Thus, the PI/LL ratio is between 0.46 and 0.49 in all cases (Table 2), values that have allowed an adequate granulation due to its good workability [35].

Fig. 2 shows both the external and internal appearance of the 36 types of aggregates initially sintered. The differential factor in the color change of the aggregates has been the incorporation of pyrite. Thus, those aggregates without P (mixtures P1 to P10), are completely white. However, the incorporation of FeS₂ has given rise to a dark mottling. These blackish spots are more dispersed when the proportion of P is relatively low (aggregates from mixtures P11 to P22, with 3.75–7.5 wt% P). However, dark mottling is much more widespread when P ranges from 11.25 to 15 wt% (P23 to P36), so it could lead to think that the mineral matrix is completely dark. However, the latter is ruled out in Fig. 3, showing as examples the aggregates P18 (7.5 wt% P) and P36 (15 wt% P). It can be seen that the black mottling related to the addition by pyrite occurs only at a local level, without affecting other areas of the matrix where its concentration is probably nil or very low. Such black spots are most likely associated with the different thermal reactions occurring when this mineral is heated, especially in the range 400–800 °C (Fig. 4b). According to Földvári [23], depending on the amount of oxygen available different overlapped reactions of oxidation (exothermic), disproportion (endothermic) and/or of thermal dissociation (endothermic) can occur, giving rise to different products such as Fe₃O₄, Fe₂O₃, Fe₂(SO₄)₃, SO₃(g), SO₂(g), S and FeS. The mainly blackish coloration of the aggregate spots seems to indicate that the compounds formed have a low degree of oxidation, so it is expected that they are rich in Fe₃O₄, FeO or FeS, while the formation of Fe₂O₃ (associated with reddish colors) is expected to be minor or non-existent.

The properties of the ceramic aggregates obtained from the starting formulations are shown in Table 3. The skewness values close to zero in all properties is an indicator that the distribution of the data shows a high degree of symmetry. On the other hand, the somewhat negative kurtosis values observed for all the variables, except for P_C and S, suggest a slightly platykurtic (flattened) distribution. In the case of P_C , the positive kurtosis would indicate that the distribution is leptokurtic (tending to be sharp), while the value equal to 0 in S is typical of a normal distribution. However, the kurtosis values are generally very close to zero for all measured properties, which is indicative of a distribution tending towards normality.

The coefficients of variation are generally relatively low, with the greatest dispersion in the data series corresponding to WA_{24} , P_O , P_C and S (CV > 39%). Greater dispersion is indicative of greater variability of properties in the aggregates obtained. With respect to the firing temperature (Table 3), there are two groups of samples. On the one hand, those mixtures that have withstood temperatures equal to or higher than 1330 °C (the majority) and, on the other hand, those fired between 1200 and 1295 °C (P5, P9, P10, P13, P14, P19, P21, P22, P25, P26, P33, P34 and P36). The latter are characterized by the highest proportions of N (3.75–5 wt%), which, as expected, has acted as a flux, substantially reducing the working temperature.

In line with Moreno-Maroto et al. [16], the greatest mass loss during heating occurs during preheating (Table 3). Regarding the total LOI during sintering of the aggregates, the minimum value was measured in mixture P1 ($LOI_{firing} = 12.8\%$) and the maximum in P36 ($LOI_{firing} =$

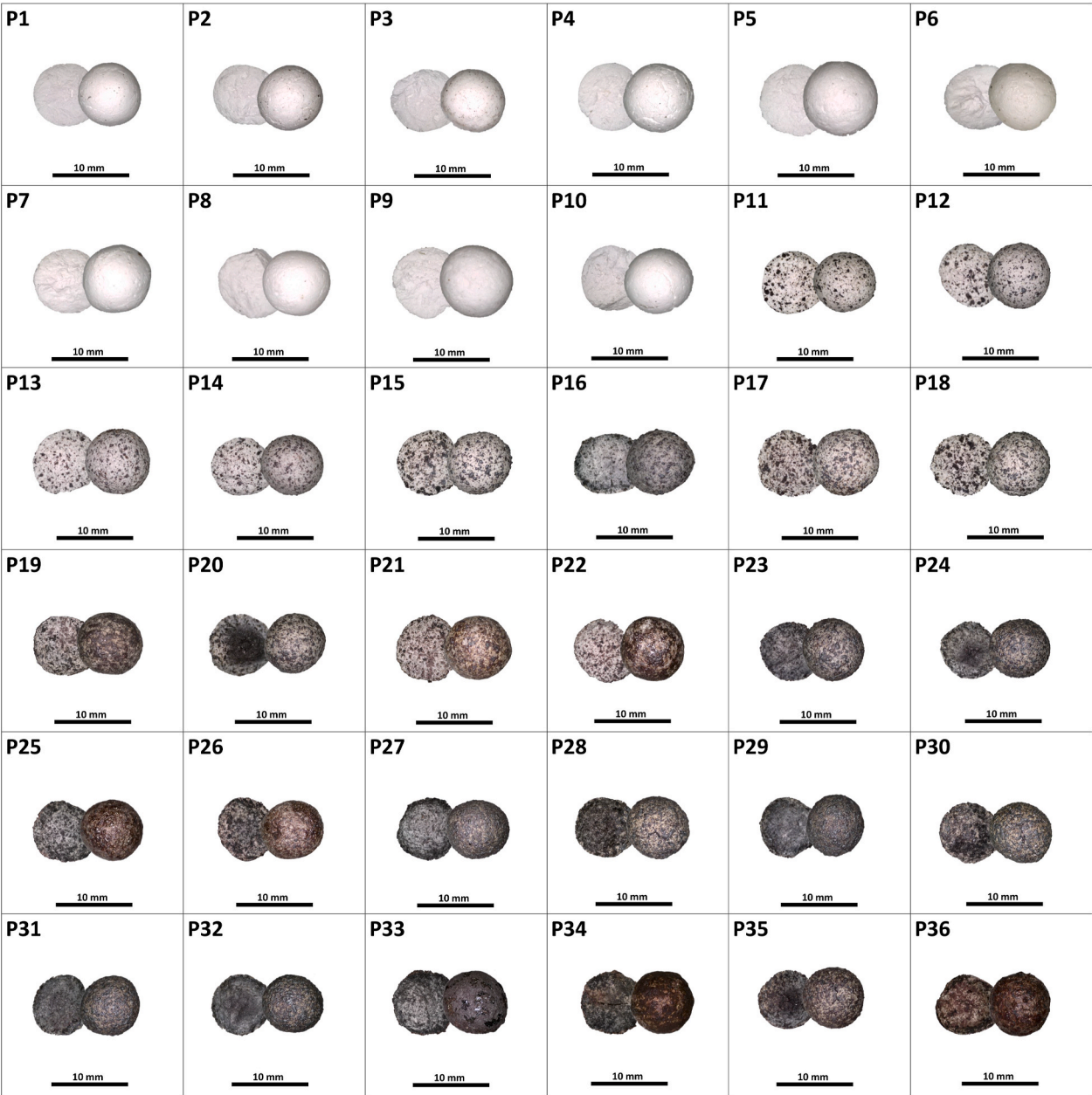


Fig. 2. Outer face and core of the 36 varieties of aggregate initially obtained to prepare the statistical models.

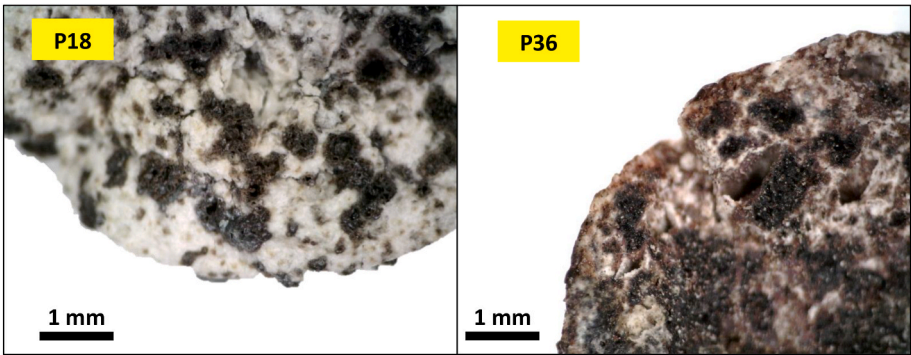


Fig. 3. Interior detail views of the sintered aggregates from the P18 and P36 mixtures.

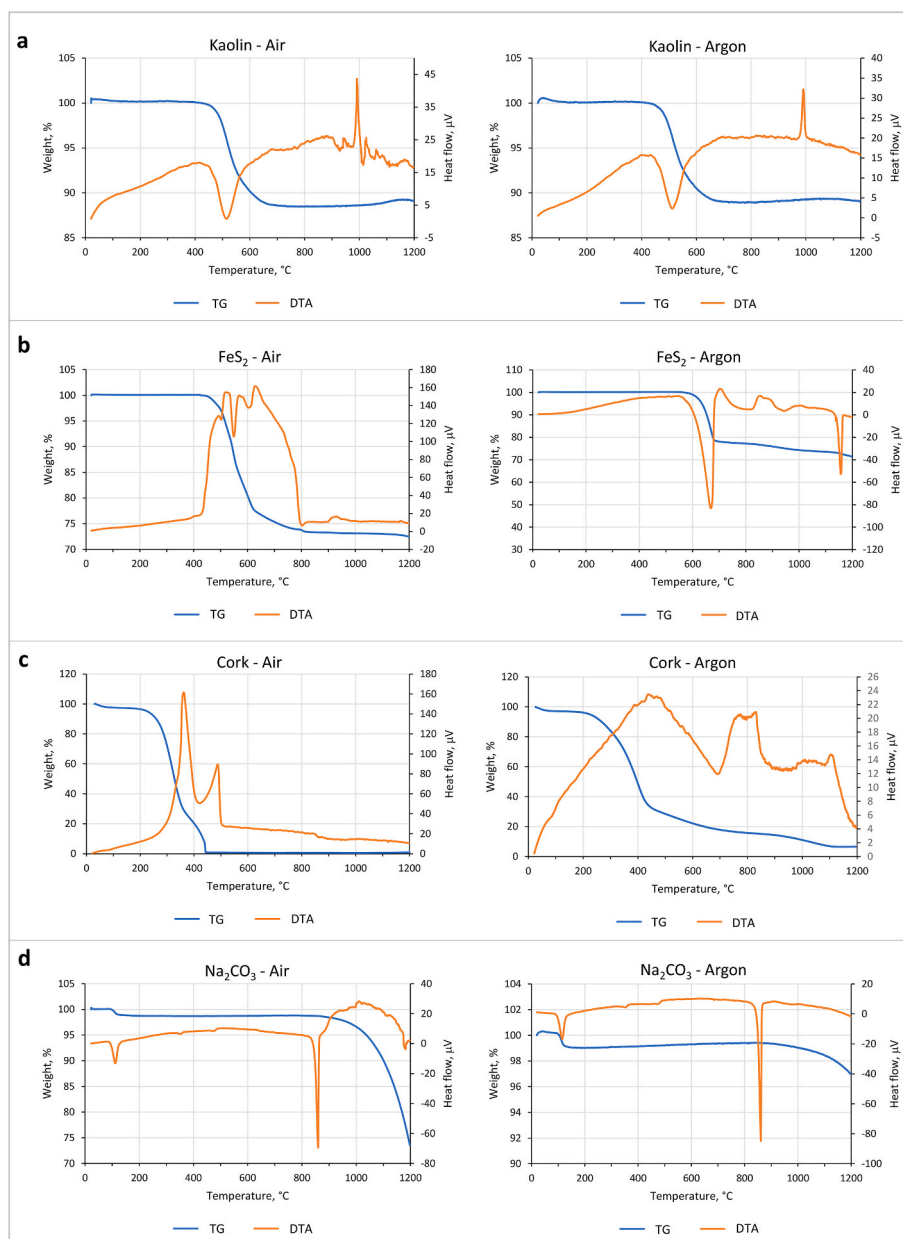


Fig. 4. DTA-TG graphs in air and Ar atmosphere for the primary components of the mixtures: (a) kaolin; (b) pyrite; (c) cork powder; (d) sodium carbonate.

21.5%). The former contains only kaolin, while the latter has 15 wt% P + 5 wt% C + 5 wt% N. Based on Földvári [23], the graphs in Fig. 4 show that the main sources of gases responsible for this LOI are, to a lesser degree: 1) the endothermic dehydroxylation of kaolin between 400 and 600 °C to form $\text{H}_2\text{O}(\text{g})$ (Fig. 4a); and to a greater extent: 2) the exothermic oxidation of FeS_2 to release SO_2 and/or SO_3 between 400 and 800 °C (Figs. 4b), 3) the exothermic oxidation of cork between approx. 250–500 °C releasing CO_2 and/or CO and $\text{H}_2\text{O}(\text{g})$ (Fig. 4c) and 4) the endothermic dissociation of Na_2CO_3 above 850 °C to release CO_2 (Fig. 4d). With respect to the oxidation of pyrite indicated above, Fe_2O_3 could be formed, which later, through the intermediation of CO and/or pure carbon from incomplete combustion of the cork, could lead to its reduction to Fe_3O_4 and/or FeO , with the consequent release of O_2 [36].

3.1.2. Main technological properties of the aggregates

Although in all varieties there has been a decrease in aggregate diameter with respect to the unfired pellet (resulting in negative BI values; Table 3), the data for both ρ_b and ρ_{rd} show that almost all

mixtures have yielded *lightweight aggregates* (LWAs) according to the EN-13055-1 [37]. Considering the maximum limit of 1.20 g/cm^3 for ρ_b and 2.00 g/cm^3 for ρ_{rd} established by this standard, the specimens corresponding to the mixtures P23, P31, P32 and P33 would not meet the second of these criteria. Despite this, they can be considered as *lightweight* since their ρ_b results are slightly lower than 1.20 g/cm^3 . However, the aggregates obtained from P3, P16, P27 and P29 would exceed both threshold values, so they cannot be categorized as LWAs in any case. The heaviest aggregate is that of P27 ($\rho_b = 1.28 \text{ g/cm}^3$ and $\rho_{rd} = 2.28 \text{ g/cm}^3$), whose mixture contains neither C nor N, but 15 wt% pyrite. For its part, the lightest one corresponds to the P10 mixture ($\rho_b = 0.83 \text{ g/cm}^3$ and $\rho_{rd} = 1.47 \text{ g/cm}^3$), which contrary to the previous one contains no P, but 5 wt % of C and N. Although most of the aggregates obtained are lightweight, they do not present the typical structural differentiation formed by an outer shell and a core of different color (Figs. 2 and 3), because as mentioned in Section 3.1.1, the process of pore formation by oxidation, disproportion and thermal dissociation of the pyrite (Fig. 4b; [23]) occur at a local level throughout the entire body of the sintered specimen (i.e.,

Table 3

Main characteristics of the aggregates obtained from the starting formulations.

Mixture	T (°C)	Ø (mm)	BI (%)	LOI _{rotary kiln} (%)		Density (g/cm ³)				WA ₂₄ (%)	Porosity, P (%)			S (MPa)
				LOI _{preh}	LOI _{firing}	ρ _b	ρ _a	ρ _{rd}	ρ _{solid} ^a		P _T	P _O	P _C	
P1	1345	8.3	−9.1	11.3	12.8	1.10	2.58	1.94	2.60	12.6	25.3	24.6	0.6	9.7
P2	1345	8.4	−8.3	14.1	14.9	0.98	2.33	1.75	2.60	14.3	32.8	25.0	7.9	7.3
P3	1345	8.2	−11.3	11.3	12.9	1.22	2.50	2.14	2.60	6.7	17.6	14.3	3.4	18.1
P4	1345	8.7	−7.9	15.6	17.2	0.88	2.12	1.52	2.60	18.5	41.4	28.2	13.2	5.5
P5	1260	8.7	−7.1	12.2	14.9	0.98	2.43	1.75	2.60	16.1	32.9	28.2	4.7	7.9
P6	1330	8.2	−11.3	14.9	15.9	1.06	2.25	1.88	2.60	8.8	27.7	16.5	11.2	12.3
P7	1330	8.3	−10.3	15.1	16.0	1.08	2.26	1.91	2.60	8.1	26.5	15.6	10.9	12.5
P8	1330	8.2	−12.4	16.0	17.6	0.99	2.08	1.75	2.60	9.2	32.8	16.2	16.6	9.6
P9	1250	8.7	−7.2	14.4	16.6	0.88	2.21	1.58	2.60	18.0	39.3	28.5	10.9	5.0
P10	1230	8.7	−7.9	17.5	18.4	0.83	2.14	1.47	2.60	21.4	43.6	31.6	12.0	3.8
P11	1345	8.3	−9.8	11.4	15.3	1.08	2.25	1.94	2.69	7.1	28.0	13.7	14.3	9.4
P12	1345	8.3	−10.2	14.7	17.3	1.01	2.13	1.76	2.69	9.9	34.7	17.5	17.2	7.9
P13	1295	8.5	−8.0	13.3	16.0	1.02	2.21	1.83	2.69	9.4	32.2	17.3	15.0	7.6
P14	1265	8.3	−9.4	16.1	17.9	0.95	2.11	1.64	2.70	13.7	39.3	22.5	16.7	7.1
P15	1345	8.6	−7.5	13.2	14.5	1.12	2.33	2.00	2.78	7.1	28.2	14.2	13.9	8.9
P16	1345	8.2	−11.1	14.0	15.0	1.28	2.38	2.26	2.78	2.2	18.9	5.0	13.9	15.3
P17	1345	8.7	−6.3	13.5	16.8	0.92	2.15	1.67	2.78	13.4	40.0	22.5	17.5	6.1
P18	1340	8.4	−8.1	15.3	18.7	0.86	2.08	1.58	2.79	15.3	43.5	24.2	19.3	7.0
P19	1220	8.7	−5.9	14.0	15.9	1.04	2.26	1.83	2.79	10.3	34.2	18.9	15.3	8.0
P20	1340	8.1	−13.6	16.3	19.6	1.05	2.02	1.81	2.79	5.7	35.2	10.3	24.9	11.1
P21	1215	9.0	−5.2	14.2	18.1	0.95	2.20	1.64	2.79	15.7	41.5	25.8	15.7	4.2
P22	1210	8.5	−9.1	16.1	20.2	0.89	2.13	1.56	2.80	17.2	44.3	26.9	17.4	5.0
P23	1340	8.2	−11.6	15.4	16.4	1.19	2.34	2.15	2.88	3.9	25.4	8.4	16.9	10.6
P24	1340	8.1	−12.4	15.6	19.1	1.04	2.14	1.91	2.88	5.7	33.7	10.9	22.9	9.0
P25	1250	8.4	−10.2	11.4	17.3	1.16	2.30	2.02	2.88	6.1	30.1	12.4	17.7	8.0
P26	1230	8.4	−9.5	13.0	19.6	0.99	2.09	1.75	2.89	9.2	39.4	16.2	23.2	9.2
P27	1340	8.3	−10.4	12.6	15.8	1.28	2.48	2.28	2.96	3.4	22.9	7.8	15.1	14.3
P28	1340	8.4	−8.5	14.1	19.0	1.02	2.06	1.79	2.97	7.2	39.7	12.9	26.8	11.4
P29	1340	8.2	−10.1	11.9	16.0	1.27	2.38	2.27	2.97	2.1	23.6	4.7	18.9	17.8
P30	1340	8.3	−10.5	19.1	21.2	0.93	1.96	1.70	2.98	7.7	42.9	13.2	29.7	11.4
P31	1340	8.0	−13.2	15.8	18.6	1.18	2.27	2.09	2.98	3.9	29.9	8.2	21.7	15.6
P32	1340	8.1	−12.8	15.8	18.6	1.17	2.22	2.04	2.98	4.1	31.6	8.4	23.3	14.6
P33	1230	8.6	−6.9	13.2	17.3	1.11	2.34	2.07	2.98	5.5	30.6	11.4	19.1	8.6
P34	1215	8.5	−8.2	15.8	20.2	0.98	2.15	1.77	2.99	9.8	40.7	17.5	23.2	6.3
P35	1340	8.1	−13.3	17.2	21.0	1.05	2.07	1.85	2.99	5.8	38.2	10.8	27.4	9.4
P36	1200	8.5	−10.1	16.0	21.5	0.88	2.05	1.59	3.00	14.4	47.2	22.8	24.3	5.2
Max	1345	9.0	−5.2	19.1	21.5	1.28	2.58	2.28	3.00	21.4	47.2	31.6	29.7	18.1
Min	1200	8.0	−13.6	11.3	12.8	0.83	1.96	1.47	2.60	2.1	17.6	4.7	0.6	3.8
Mean	1303	8.4	−9.6	14.5	17.3	1.04	2.22	1.85	2.79	9.7	33.8	17.0	16.7	9.5
St. Dev.	53.4	0.2	2.2	1.9	2.2	0.12	0.14	0.22	0.15	5.1	7.5	7.3	6.6	3.7
CV (%)	4	3	−23	13	13	12	7	12	5	52	22	43	40	39
Kurtosis	−1.1	−0.3	−0.7	−0.2	−0.5	−0.6	−0.2	−0.6	−1.5	−0.6	−0.7	−1.0	0.2	0.0
Skewness	−0.8	0.4	−0.1	0.0	0.0	0.3	0.5	0.4	0.0	0.5	−0.3	0.2	−0.3	0.7

^a Estimated value according to Eq. (1).

the reactions occurring on the outside and inside of the aggregate would be practically the same). This contrasts with the literature, which show the suitability of pyrite as a bloating agent in LWAs [13]. As indicated in section 2.2, the maximum amount of pyrite applied was 15 wt% because higher proportions could lead to significant emissions of harmful gases such as SO₂ and SO₃, making the experimental protocol unsafe and not feasible. Therefore, taking this into account, the results obtained do not allow completely ruling out that the incorporation of higher pyrite proportions (or of the other additives) could lead to volumetric expansion. This aspect would involve additional research to be conducted under controlled conditions, something that is beyond the scope of this research, especially considering that this work focuses on the synthesis under statistical criteria of ceramic granular materials, regardless of whether they are finally lightweight or not.

As can be seen in Fig. 5a, the decrease in density is directly linked to the increase in porosity. In this sense, porosity will also influence other parameters. In the case of water absorption, it is clear from Fig. 5b that P_O and WA₂₄ grow together as they express the same information but in different ways (volume vs mass, respectively). The mixture with the aggregate showing the highest WA₂₄ is P10 (WA₂₄ = 21.4%). P10 specimens present the highest percentage of open pores in this study (P_O = 31.6%), which would be associated with the voids left by both C and N upon thermal decomposition. The most watertight aggregate is P29

(WA₂₄ = 2.1%), whose open porosity is the lowest of all (P_O = 4.7%).

From a mechanical point of view, the lowest value of S is that of the aggregate manufactured from the P10 mixture (S = 3.8 MPa), which is in turn the lightest and most porous variety of all. On the other hand, P3 is the aggregate with the highest crushing strength (S = 18.1 MPa) and the lowest porosity (P_T = 17.6%). Therefore, there is an inverse relationship between porosity and mechanical strength (Fig. 5c). However, there are a number of varieties (gray colored dots in Fig. 5c) that present higher S values than expected according to the trend line obtained. These varieties correspond to certain aggregates with high pyrite contents: P18 and P20 (P = 7.5 wt%), P26 (P = 11.25 wt%), P28, P29, P30, P31, P32 and P35 (P = 15 wt%). Therefore, these data suggest that the incorporation of pyrite may contribute to a stronger structure. The causes that could lead to this higher mechanical strength when the pyrite proportion is high may be several. For example, it could be linked to the development of a denser and more compact mineral matrix, or to the neoformation of harder mineral species. To find this out, a specific investigation would be required, which exceeds the objectives of this work.

3.2. Modeling: Analysis of effect and response surface plots

Once the aggregate characterization results were known (Table 3),

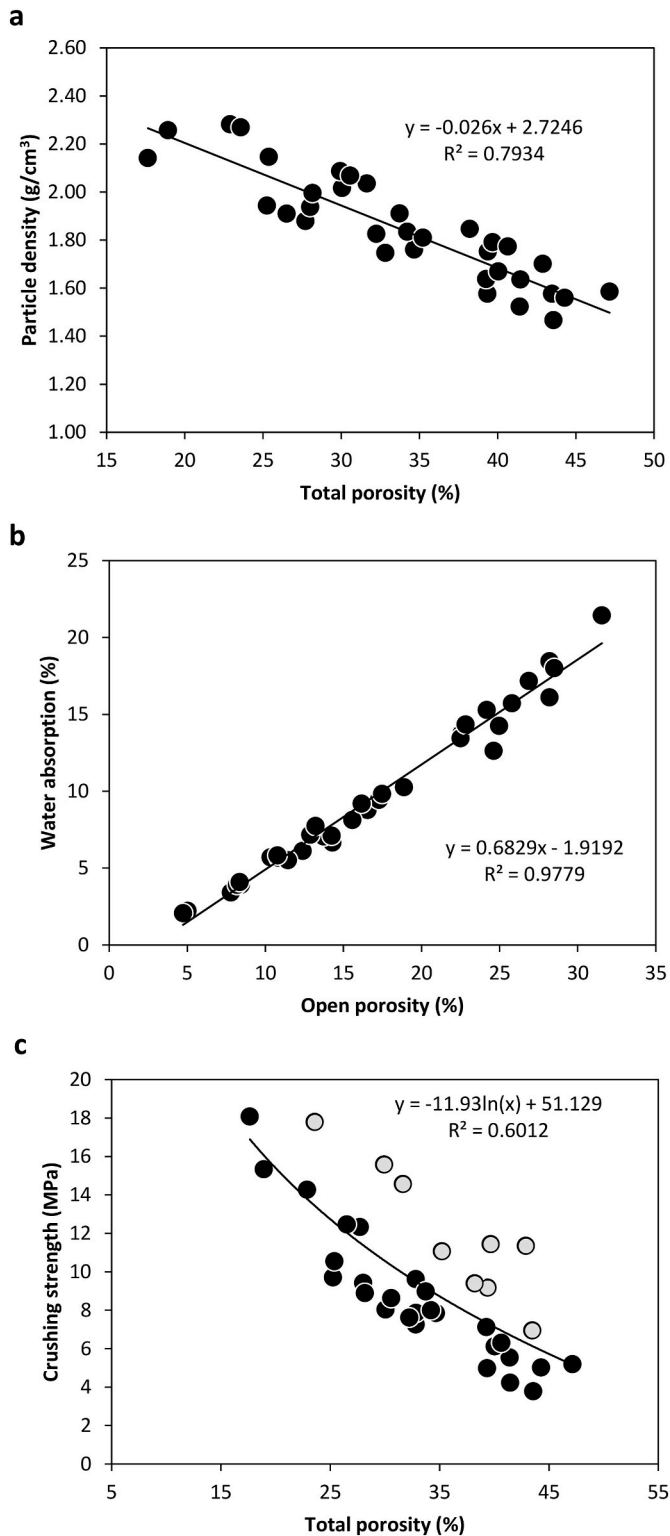


Fig. 5. Influence of porosity on other technological properties: (a) P_T vs ρ_{rd} ; (b) P_O vs WA_{24} ; (c) P_T vs S . The gray dots in (c) show an anomalously higher crushing strength than expected based on their porosity.

the best fitting models for BI , ρ_{rd} , WA_{24} and S were searched for. Table 4 shows the properties and the coefficients of the regression models. The best fit is a quadratic model, except for WA_{24} where the most appropriate approach is the cubic one. The four models obtained are statistically significant and with a high coefficient of determination ($R^2 = 0.852$ – 0.978 ; Table 4), which a priori would lead to a good predictive

Table 4

Coefficients of the regression models and analysis of variance obtained for each key property.

	BI (quadratic)	ρ_{rd} (quadratic)	WA_{24} (cubic)	S (quadratic)
K	−8.8	2.0	11.9	10.4
P	−169.4	10.2	3007.1	384.0
C	−1293.9	99.0	−57744.0	2231.8
N	5881.2	−372.4	−124127.9	−8082.3
cubic (K, P)	−	−	1964.2	−
cubic (K, C)	−	−	−30685.0	−
cubic (K, N)	−	−	−73218.7	−
cubic (P, C)	−	−	−30219.8	−
cubic (P, N)	−	−	−49360.2	−
cubic (C, N)	−	−	−87744.0	−
K:P	183.4	−7.8	−4965.0	−410.7
K:C	1366.4	−110.7	88548.2	−2432.6
K:N	−6153.3	389.9	196660.0	8494.5
P:C	1320.6	−136.7	78109.8	−2743.0
P:N	−5903.8	384.8	171486.1	7614.4
C:N	−5750.2	327.2	339021.3	5992.8
K:P:C	−	−	−51172.6	−
K:P:N	−	−	−120827.9	−
K:C:N	−	−	−268196.9	−
P:C:N	−	−	−223284.3	−
F-test	420.9	4304.0	177.3	133.2
p-value	2.20E-16	2.20E-16	3.89E-15	2.20E-16
R^2	0.873	0.955	0.978	0.852

capacity. This last aspect will be addressed in Section 3.3. The response surface plots (whose feasible area is the rhombus delimited by the dashed line appearing in each figure) and effect plots are shown in Fig. 6 and Fig. 7, respectively. These will be discussed together.

Figs. 6a and 7a refer to BI . First, it should be noted that, as indicated in Section 3.1.2, the volumetric variation has been negative in all cases. That is, bloating has not occurred, or it has not been large enough to exceed the size of the starting pellet. Therefore, the discussion of BI from now on will simply allude to the shrinkage that the specimen has undergone during firing (i.e., higher values of BI indicate lower volumetric shrinkage, and vice versa). Analyzing component by component, Fig. 7a shows that BI increases directly with kaolin content and inversely with the proportion of pyrite added. In the case of organic matter (whose centroid in Fig. 7a is located at $C = 2.5$ wt%), shrinkage is inhibited to some extent at values of about 1 wt% C, a threshold that when exceeded leads to a decrease in BI . In the case of N, two effects are detected which appear to be opposed. Thus, BI tends to be higher in the absence of sodium carbonate, or on the contrary, when it reaches its highest percentage ($N = 5$ wt%), while in intermediate ranges (especially around the centroid: 2.5 wt% N), the aggregate shrinkage is favored.

In the case of ρ_{rd} and S , the trends are similar (Fig. 6b,d and Fig. 7b,d), so they can be discussed in parallel. Both properties tend to be higher with increasing the percentages of kaolin and especially pyrite in the formulations, while the incorporation of C affects them negatively. Therefore, what determines higher strength and density are mainly the presence of P and the absence of C. Contrary to what happened with BI , the higher S and ρ_{rd} values would be linked to intermediate N percentages (approx. $N = 2.5$ wt%).

Regarding water absorption (Figs. 6c and 7c), the addition of P clearly decreases this property, while the opposite occurs with the addition of C, probably due to the formation of open pores as the cork decomposes. In the case of N, as with BI , the increase in WA_{24} requires either no addition of N (perhaps inhibiting the formation of a liquid phase that could clog the micropores formed during sintering), or an addition of around 5 wt% of N (something that could probably favor the

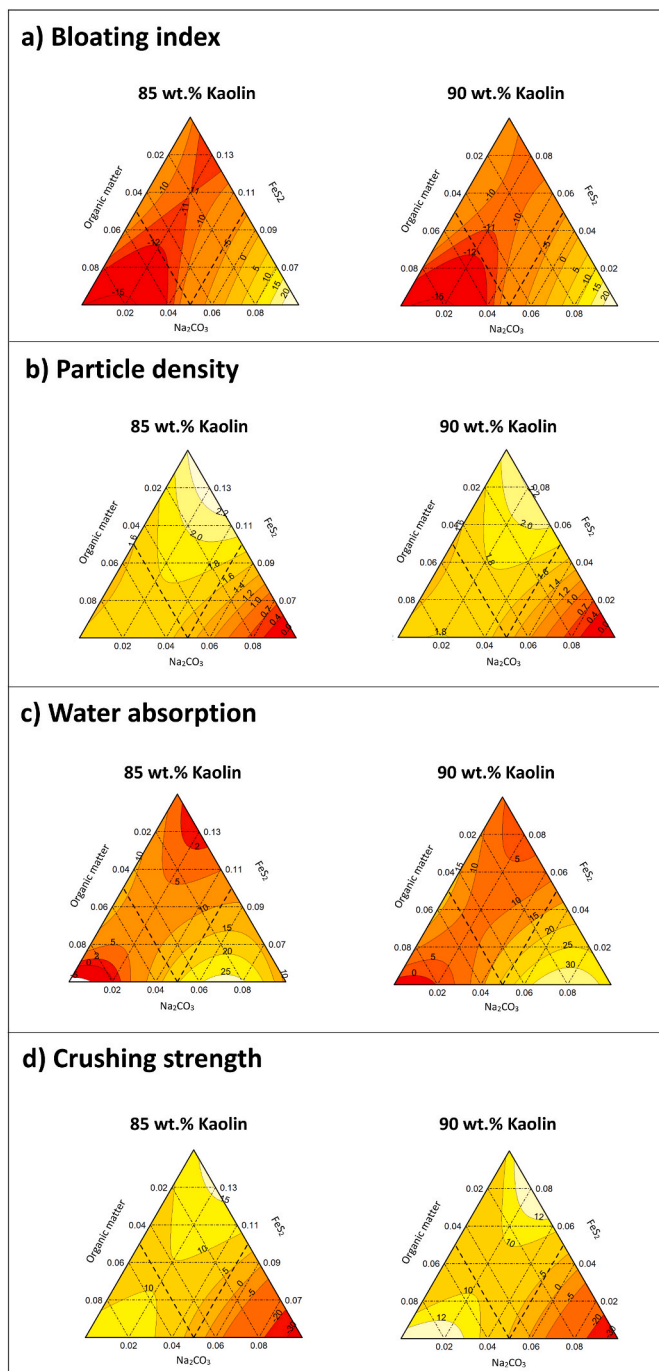


Fig. 6. Response surface plots for 85 and 90 wt% kaolin: (a) bloating index; (b) particle density; (c) water absorption; (d) crushing strength.

formation of larger open pores, capable of harboring water). In the case of kaolin, something similar to the trends for sodium carbonate occurs, whereby the absorptive capacity of the aggregates seems to be higher either when the kaolin content in the mixture is relatively low ($K < 80$ wt%) or high ($K > 90$ wt%), but lower in intermediate ranges.

3.3. Optimization and model validation

Based on the models in Table 4, the four key properties under analysis have been optimized. Specifically, the mixtures with the maximum values of BI , WA_{24} and S and, on the other hand, minimum ρ_{rd} , have been estimated, as shown in Table 5, whose aggregates are

shown in Fig. 8. Thus, Table 5 includes the experimentally observed values of these optimal mixtures, as well as the estimated values and their confidence intervals provided by the models. Considering percentages by weight, for the bloating index, its theoretical optimum would be reached with the Op-1 mixture: 87.6% K + 6.7% P + 0.7% C + 5.0% N. The BI value estimated for this formulation is $BI = -5.6\%$, very similar to that measured experimentally when testing its aggregates in the laboratory ($BI = -5.8\%$), and in the same order as the minimum recorded in the previous variants (minimum BI of -5.2% in P21), which seems to indicate that this optimum is very well estimated.

In the case of Op-2 (88.2% K + 1.8% P + 5.0% C + 5.0% N), which seeks the minimum density, again the estimated and experimental values (in this case for ρ_{rd}) are almost coincident with each other (ρ_{rd} of 1.48 and 1.46 g/cm³, respectively), and with the minimum obtained in the preliminary tests (1.47 g/cm³ in P10; Table 3). Following the same parallelism, the Op-3 blend (90%K + 0.0%P + 5.0%C + 5.0%N, which coincides with blend P10 in Table 3) presents data that in practice are similar for WA24: 21.2% absorption as estimated maximum and 21.4% according to experimental data.

Op-4 is the mixture that has been estimated to maximize the mechanical strength, whose composition is 83.0% K + 15.0% P + 0.0% C + 2.0% N. The difference between the estimated value ($S = 17.3$ MPa) and the laboratory tested value ($S = 15.3$ MPa) is only 2 MPa. Although somewhat lower, this result is also in the same order as that recorded for variety P3 ($S = 18.1$ MPa; Table 3).

As can be seen in Table 5, the rest of the estimated results of BI , WA_{24} , S and ρ_{rd} , for each of the optimum mixtures are almost coincident with those obtained by contrasting them experimentally. In addition, in all cases the experimentally observed values are within the confidence intervals. These aspects demonstrate that the four statistical models fit properly, allowing very accurate predictions of the technical properties of the mixtures. This fact is especially relevant, considering that the mixtures have contained four components with very different characteristics (K, P, C and N), whose synergies would be practically unpredictable if the ME-DOE had not been applied. Therefore, it is shown that this statistical approach can have enormous potential in the optimization and prediction of multicomponent mixtures for ceramic materials, such as the synthetic aggregates of this research.

4. Conclusions

First, from a more particular perspective, it has been observed that each of the components of the mixtures are critical depending on the final characteristics to be obtained:

- Contrary to expectations, the thermal decomposition of pyrite has not produced any significant volumetric expansion in the aggregates for the proportions studied. Greater amounts of P in the mixtures has favored an increase in density, mechanical strength and volumetric shrinkage, while the water absorption capacity of the aggregate decreased.
- The incorporation of organic matter in the mixtures in the form of cork powder (C), only seems to have significantly favored the increase in water absorption (WA_{24}), while the rest of the measured parameters (BI , ρ_{rd} , S) generally tend to decrease with increasing C content.
- Sodium carbonate (N), apart from helping to reduce the sintering temperature, is characterized by the fact that in its average percentage (2.5 wt%, since it has been studied between 0 and 5 wt%) is where the maximum (concave trend) or minimum (convex trend) is found, depending on the property studied. For crushing strength and particle density, the first of the cases would occur (maximum at 2.5 wt% of N), while the opposite occurs for water absorption and bloating index (minimum at 2.5 wt% of N).
- Higher percentages of kaolin are also associated with higher values in the four properties studied, although in the case of water

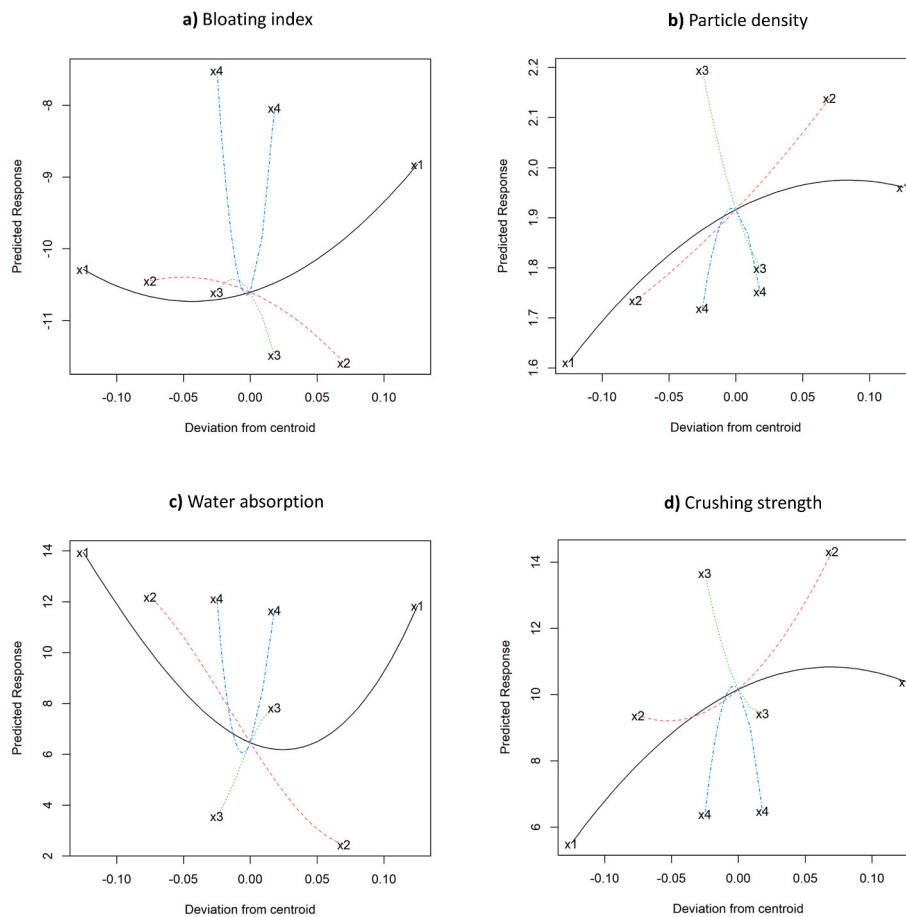


Fig. 7. Effect plots for: (a) bloating index; (b) particle density; (c) water absorption; (d) crushing strength. Where: x1 = % kaolin; x2 = % FeS₂; x3 = % organic matter (cork); x4 = % Na₂CO₃.

Table 5

Optimal formulations and comparison between experimentally determined and statistically model-estimated properties. Confidence intervals for the estimated values are shown in parentheses.

Optimum formulation		Bloating index (%)			Particle density (g/cm ³)			Water absorption (%)			Crushing strength (MPa)		
		Exp.	Est.	Dif.	Exp.	Est.	Dif.	Exp.	Est.	Dif.	Exp.	Est.	Dif.
Op-1 (for max <i>BI</i>)	87.6%K + 6.7%P + 0.7%C + 5.0%N	−5.8	−5.6 (−7.7, −3.5)	0.2	1.73	1.76 (1.64, 1.88)	0.03	13.1	11.7 (8.8, 14.5)	−1.4	5.9	5.7 (1.9, 9.4)	−0.2
Op-2 (for min ρ_{rd})	88.2%K + 1.8%P + 5.0%C + 5.0%N	−7.3	−8.2 (−10.3, −6.0)	−0.9	1.46	1.48 (1.35, 1.61)	0.02	19.9	21.0 (18.0, 23.9)	1.1	4.3	3.7 (−0.3, 7.7)	−0.6
Op-3 (for max <i>WA</i> ₂₄)	90%K + 0.0%P + 5.0%C + 5.0%N	−7.9	−8.4 (−10.6, −6.1)	−0.5	1.47	1.48 (1.34, 1.61)	0.01	21.4	21.2 (18.1, 24.3)	−0.2	3.8	4.6 (0.5, 8.7)	0.8
Op-4 (for max <i>S</i>)	83.0%K + 15.0%P + 0.0%C + 2.0%N	−10.8	−12.1 (−14.2, −10.0)	−1.3	2.28	2.37 (2.25, 2.50)	0.09	2.6	0.9 (−2.1, 3.8)	−1.7	15.3	17.3 (13.4, 21.2)	2.0

absorption, there is also an even more notable increase when its proportion is low (convex trend).

As a general conclusion, it has been demonstrated that the application of ME-DOE statistical methodology exhibits the following advantages:

- Although the mixtures are multicomponent (in this case 4 components: K, P, C and N), ME-DOE allows a very significant reduction in the number of laboratory tests (in this case only 36 starting mixtures were necessary), thus saving time and resources.
- Obtaining models with a good fit with respect to the real behavior measured in the laboratory (as it has happened in this case), allows the technological changes of the materials (in this research, artificial aggregates) to be understood with great precision with respect to the

components of the formulations from which they originate. In this sense, response surface plots and effect plots are very useful tools.

- In this work it is also demonstrated that the last step, optimization, is very accurate with ME-DOE. This is especially advantageous when the aim is to maximize or minimize a certain characteristic of the product to be obtained, paving the way for the development of tailor-made artificial aggregates.

CRediT authorship contribution statement

José Manuel Moreno-Maroto: Conceptualization, Data curation, Formal analysis, Investigation, Methodology, Supervision, Validation, Visualization, Writing – original draft, Writing – review & editing, Funding acquisition, Project administration. **Carlos Javier Cobo-Ceacero:** Investigation, Writing – review & editing. **Antonio Conde-**

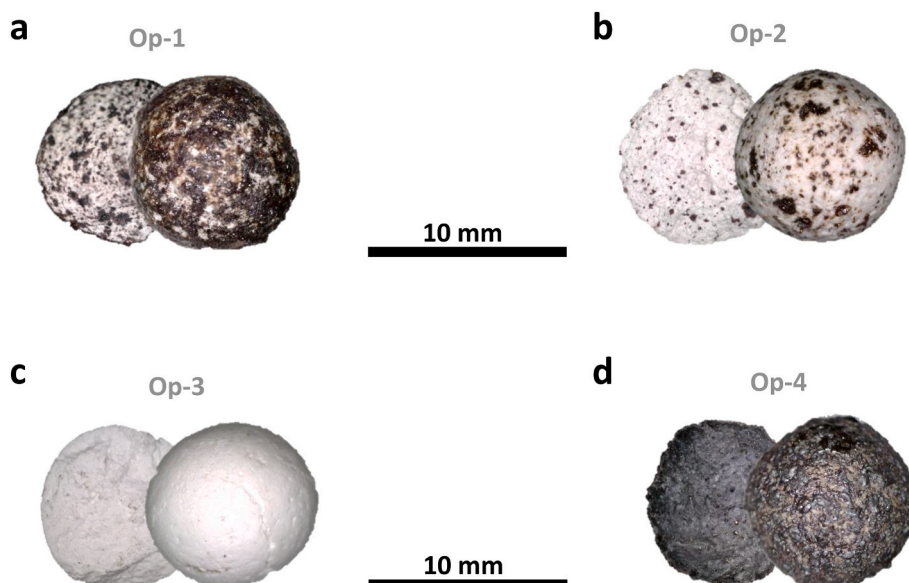


Fig. 8. Outer face and core of the 4 optimal varieties of aggregate obtained according to the statistical models: (a) Op-1 for maximum bloating index; (b) Op-2 for minimum density; (c) Op-3 for maximum water absorption; (d) Op-4 for maximum crushing strength.

Sánchez: Software, Data curation, Formal analysis, Methodology, Writing – review & editing. **Ana M. Martínez-Rodríguez:** Software, Data curation, Formal analysis, Methodology, Writing – review & editing. **Beatriz González-Corrochano:** Investigation, Writing – review & editing. **Jacinto Alonso-Azcárate:** Conceptualization, Investigation, Methodology, Supervision, Validation, Writing – review & editing, Funding acquisition, Project administration. **Manuel Uceda-Rodríguez:** Writing – review & editing. **Ana B. López:** Writing – review & editing. **Carmen Martínez-García:** Conceptualization, Investigation, Methodology, Supervision, Validation, Writing – review & editing, Funding acquisition, Project administration. **Teresa Cotes-Palomino:** Conceptualization, Investigation, Methodology, Supervision, Validation, Writing – review & editing, Funding acquisition, Project administration.

Declaration of competing interest

The authors declare that they have no known competing financial interests or personal relationships that could have appeared to influence the work reported in this paper.

Acknowledgments

This research was conducted as a part of the ECO-MET-AL Project, PID2019-109520RB-I00 / AEI / 10.13039/501100011033, “Can industrial and mining metalliferous wastes produce green lightweight aggregates? Applying the Circular Economy” funded by the Spanish Ministry of Science, Innovation and Universities and ERDF funds, framed in the “Ayudas a “Proyectos I + D + i” en el marco de los Programas Estatales de Generación de Conocimiento y Fortalecimiento Científico y Tecnológico del Sistema de I + D + i y de I + D + i orientada a los Retos de la Sociedad, Convocatoria 2019”. Thanks also to the SCAI of the University of Jaén, the University of Castilla-La Mancha and the University of Málaga for their services.

References

- [1] European Commission, Communication from the Commission to the European Parliament, the Council, the European Economic and Social Committee and the Committee of the Regions. Closing the Loop - an EU Action Plan for the Circular Economy, 2015. COM/2015/0614 final.
- [2] European Commission, COM/2020/98 Final. Communication from the Commission to the European Parliament, the Council, the European Economic and Social Committee and the Committee of the Regions. A New Circular Economy Action Plan for a Cleaner and More Competitive Europe, 2020.
- [3] European Commission, A European Green Deal, 2019. June 2022), https://ec.europa.eu/info/strategy/priorities-2019-2024/european-green-deal_en.
- [4] United Nations, 2030 Agenda for Sustainable Development. 17 Goals to Transform Our World, 2017. June 2022), <https://www.un.org/sustainabledevelopment/>.
- [5] R.R. Menezes, H.G. Malzac Neto, L.N.L. Santana, H.L. Lira, H.S. Ferreira, G. A. Neves, Optimization of wastes content in ceramic tiles using statistical design of mixture experiments, *J. Eur. Ceram. Soc.* 28 (2008) 3027–3039, <https://doi.org/10.1016/j.jeurceramsoc.2008.05.007>.
- [6] M. Arsenović, A. Radojević, Ž. Jakić, L. Pezo, Mathematical approach to application of industrial wastes in clay brick production – Part I: testing and analysis, *Ceram. Int.* 41 (3) (2015) 4890–4898. Part B.
- [7] M. Arsenović, A. Radojević, Ž. Jakić, L. Pezo, Mathematical approach to application of industrial wastes in clay brick production—Part II: Optimization, *Ceram. Int.* 41 (3) (2015) 4899–4905. Part B.
- [8] B. Ayati, V. Ferrándiz-Mas, D. Newport, C. Cheeseman, Use of clay in the manufacture of lightweight aggregate, *Construct. Build. Mater.* 162 (2018) 124–131, <https://doi.org/10.1016/j.conbuildmat.2017.12.018>.
- [9] Anefa, El Sector (The Aggregate Sector in Spain), Asociación Nacional de Empresarios Fabricantes de Áridos, 2022. June 2022), <http://www.aridos.org/e-l-sector/>.
- [10] ESCSI, Expanded Shale, Clay and Slate Institute, 2022. June 2022), <https://www.escsi.org/>.
- [11] C.M. Riley, Relation of chemical properties to the bloating of clays, *J. Am. Ceram. Soc.* 34 (4) (1951) 121–128, <https://doi.org/10.1111/j.1151-2916.1951.tb11619.x>.
- [12] E.G. Ehlers, The mechanism of lightweight Aggregate formation, *Am. Ceram. Soc. Bull.* 37 (2) (1958) 95–99.
- [13] J.C. Cubaud, M. Murat, Fabricación industrial de arcilla expandida, *Silic. Ind.* 5 (1968) 145–152.
- [14] M. Dondi, P. Cappelletti, M. D’Amore, R. de Gennaro, S.F. Graziano, A. Langella, C. Raimondo, C. Zanelli, Lightweight aggregates from waste materials: reappraisal of expansion behavior and prediction schemes for bloating, *Construct. Build. Mater.* 127 (2016) 394–409, <https://doi.org/10.1016/j.conbuildmat.2016.09.111>.
- [15] J.M. Moreno-Maroto, M. Uceda-Rodríguez, C.J. Cobo-Ceacero, M. Calero de Hoces, M.A. Martín Lara, T. Cotes-Palomino, A.B. López García, C. Martínez-García, Recycling of ‘alperujo’ (olive pomace) as a key component in the sintering of lightweight aggregates, *J. Clean. Prod.* 239 (2019), 118041, <https://doi.org/10.1016/j.jclepro.2019.118041>.
- [16] J.M. Moreno-Maroto, C.J. Cobo-Ceacero, M. Uceda-Rodríguez, T. Cotes-Palomino, C. Martínez-García, J. Alonso-Azcárate, Unraveling the expansion mechanism in lightweight aggregates: demonstrating that bloating barely requires gas, *Construct. Build. Mater.* 247 (2020), 118583, <https://doi.org/10.1016/j.conbuildmat.2020.118583>.
- [17] C. Hu, L. Wang, J. Bai, L. Yang, X. Zhan, J. Gong, Optimization mixture ratio parameters of lightweight aggregates incorporating municipal solid waste incineration fly ash and electrolytic manganese residues using the Uniform Design Method, *Fresenius Environ. Bull.* 27 (12A) (2018) 9147–9155.
- [18] Y.M. Wie, K.G. Lee, K.H. Lee, T. Ko, K.H. Lee, The experimental process design of artificial lightweight Aggregates using an orthogonal array table and analysis by

- machine learning, *Materials* 13 (23) (2020) 5570, <https://doi.org/10.3390/ma13235570>.
- [19] C.J. Cobo-Ceacero, J.M. Moreno-Maroto, M. Guerrero-Martínez, M. Uceda-Rodríguez, A.B. López, C. Martínez García, T. Cotes-Palomino, Effect of the addition of organic wastes (cork powder, nut shell, coffee grounds and paper sludge) in clays to obtain lightweight aggregates, *Bol. Soc. Esp. Ceram. Vidrio* (2022), <https://doi.org/10.1016/j.bsecv.2022.02.007>. In press.
- [20] J. Cornell, *Experiments with Mixtures*, third ed., John Wiley & Sons, New York, 2002.
- [21] J. Lawson, C. Willden, Mixture experiments in R using mixexp, *Journal of Statistical Software, Code Snippets* 72 (2) (2016) 1–20, <https://doi.org/10.18637/jss.v072.c02>.
- [22] M. Bernhardt, H. Justnes, H. Tellesbø, K. Wiik, The effect of additives on the properties of lightweight aggregates produced from clay, *Cem. Concr. Compos.* 53 (2014) 233–238, <https://doi.org/10.1016/j.cemconcomp.2014.07.005>.
- [23] M. Földvári, *Handbook of Thermogravimetric System of Minerals and its Use in Geological Practice. Occasional Papers of the Geological Institute of Hungary*, 213, Geological Institute of Hungary, 2011, 978-963-671-288-4.
- [24] ASTM D 4318-10e1, *Standard Test Methods for Liquid Limit, Plastic Limit, and Plasticity Index of Soils*, Annual Book of ASTM Standards, ASTM International, West Conshohocken, PA, 2017.
- [25] J.M. Moreno-Maroto, J. Alonso-Azcárate, Plastic limit and other consistency parameters by a bending method and interpretation of plasticity classification in soils, *Geotech. Test J.* 40 (3) (2017) 467–482, <https://doi.org/10.1520/GTJ20160059>.
- [26] E. Fakhfakh, W. Hajjaji, M. Medhioub, F. Rocha, A. López-Galindo, M. Setti, F. Kooli, F. Zargouni, F. Jamoussi, Effects of sand addition on production of lightweight aggregates from tunisian smectite-rich clayey rocks, *Appl. Clay Sci.* 35 (2007) 228–237, <https://doi.org/10.1016/j.clay.2006.09.006>.
- [27] EN-1097-6, *Tests for Mechanical and Physical Properties of Aggregates. Part 6: Determination of Particle Density and Water Absorption*, European Committee for Standardization, 2013.
- [28] EN-1097-3, *Tests for Mechanical and Physical Properties of Aggregates. Part 3: Determination of Loose Bulk Density and Voids*, European Committee for Standardization, 1998.
- [29] ACI 213R-03, *Guide for Structural Lightweight-Aggregate Concrete*, American Concrete Institute, 2003.
- [30] Y. Ke, A.L. Beaucour, S. Ortola, H. Dumontet, R. Cabrilac, Influence of volume fraction and characteristics of lightweight aggregates on the mechanical properties of concrete, *Construct. Build. Mater.* 23 (8) (2009) 2821–2828, <https://doi.org/10.1016/j.conbuildmat.2009.02.038>.
- [31] C. De Santiago Buey, M. Raya García, Análisis del peso específico y porosidad de materiales porosos mediante picnometría de helio, *Ingen. Civ.* 151 (2008) 95–103. ISSN 0213-8468.
- [32] M. Bernhardt, H. Tellesbø, H. Justnes, K. Wiik, Mechanical properties of lightweight aggregates, *J. Eur. Ceram. Soc.* 33 (2013) 2731–2743, <https://doi.org/10.1016/j.jeurceramsoc.2013.05.013>.
- [33] S. Yashima, Y. Kanda, S. Sano, Relationship between particle size and fracture energy or impact velocity required to fracture as estimated from single particle crushing, *Powder Technol.* 51 (1987) 277–282.
- [34] Y. Li, D. Wu, J. Zhang, L. Chang, Z. Fang, Y. Shi, Measurement and statistics of single pellet mechanical strength of differently shaped catalysts, *Powder Technol.* 113 (1–2) (2000) 176–184, [https://doi.org/10.1016/S0032-5910\(00\)00231-X](https://doi.org/10.1016/S0032-5910(00)00231-X).
- [35] J.M. Moreno-Maroto, J. Alonso-Azcárate, What is clay? A new definition of “clay” based on plasticity and its impact on the most widespread soil classification systems, *Appl. Clay Sci.* 161 (2018) 57–63, <https://doi.org/10.1016/j.clay.2018.04.011>.
- [36] S. Toyama, M. Kawamura, On the relationship between the bloating of lightweight aggregate and reaction progress of the constituents, *J. Chem. Eng. Jpn.* 4 (3) (1971) 251–256.
- [37] EN-13055-1, *Lightweight Aggregates. Part 1: Lightweight Aggregates for Concrete, Mortar and Grout*, European Committee for Standardization, 2002.